Wang *et al. Chem. Biol. Technol. Agric.* (2022) 9:101
https://doi.org/10.1186/s40538-022-00374-4

Chemical and Biological Technologies in Agriculture

RESEARCH

Open Access

Effects of acidic phosphorus-rich biochar from halophyte species on P availability and fractions in alkaline soils

Xuyang Wang[1†], Tao Sun[2†], Haigang Ma[3], Guangmu Tang[3], Mo Chen[4], Maidinuer Abulaizi[4], Guangling Yu[1] and Hongtao Jia[1*]

Abstract

Conditioning alkaline soil with acidic phosphorus-rich biochar might contribute to improving soil phosphorous (P) availability and waste utilization efficiency. In this study, acidic phosphorus-rich biochar was prepared using halophyte biochar (HBC) modified by H_3PO_4 (P-HBC) and $H_4P_2O_7$ (PA-HBC). The P-containing groups and P fractions in the HBCs were characterized, and the effects of biochar on the P fractions in alkaline soil were examined with incubation experiments. The results showed that the pH of P-HBC (3.31) and PA-HBC (2.17) was significantly reduced compared with HBC, and the total P contents rose to 4.66 $g \cdot kg^{-1}$ and 5.24 $g \cdot kg^{-1}$, respectively. The spectral characterization confirmed the loading of P-containing and acidic functional groups in the HBCs after modification. The application of P-HBC and PA-HBC in alkaline soils decreased the soil pH and facilitated the transformation of stable P into active fractions. Overall, acidic phosphorus-rich biochar can be employed to increase P activity in alkaline soil.

Keywords: Alkaline soil, Biochar, Halophytes, Phosphorus, Modification

†Xuyang Wang and Tao Sun have equally contributed to this work

*Correspondence: jht@xjau.edu.cn

[1] College of Resources and Environment Sciences, Xinjiang Agricultural University, East Nongda Road No. 311, Urumqi 830052, China
Full list of author information is available at the end of the article

Graphical Abstract

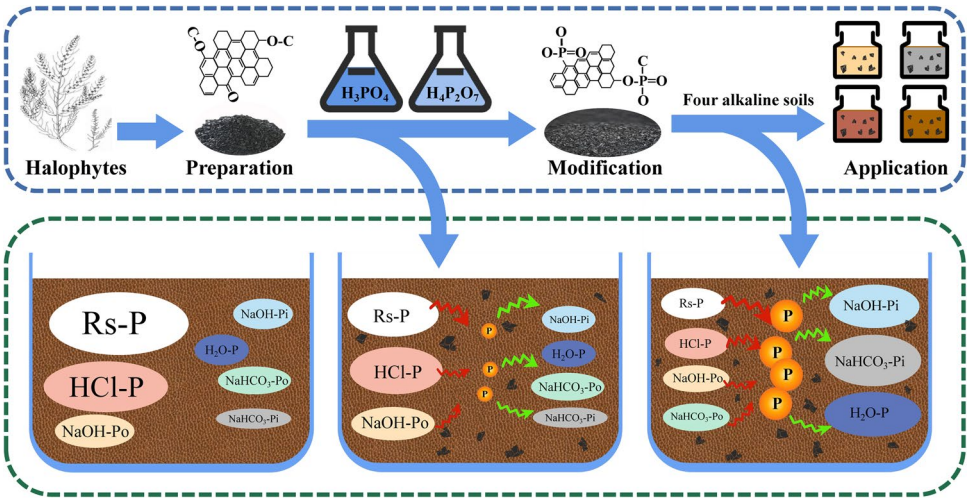

Introduction

Alkaline soils are important agricultural soil resources [1, 2]. However, the utilization efficiency of phosphorus (P) in alkaline soil is low, because P can combine with mineral elements to form insoluble compounds [3]. Previous studies reported that the availability of phosphate fertilizer was only 10–25% in Xinjiang [4]. Under the current socioeconomic and environmental requirements of sustainability, it is necessary to improve P availability in alkaline soils.

The positive effects of biochar on soil improvement have attracted increasing attention [5]. Biochar has the potential to enhance soil fertility through nutrient retention and improving the soil microenvironment [6, 7]. However, the nutrients available to plants provided by the biochar also changed with soil type when biochar was added to the soil. For example, Chen et al. [8] suggested that adding biochar to acidic soils was considered an effective way of reducing P leaching and increasing the retention of P. In contrast, P has been fixed due to the formation of precipitates between P and divalent cations (Ca^{2+} and Mg^{2+}) in alkaline soil. This leads to the reduced availability of P in alkaline soil [9, 10]. The highly exchangeable cations and pH of biochar resulted in P retention in alkaline soils [11], which limited the application of biochar in alkaline soil. Therefore, it is meaningful to find a method of modification for appropriately preparing biochar for improving P availability in alkaline soils.

Plants that adapt to living in saline soils are called halophytes. There are approximately 1560 species of halophytes in the world and more than 500 species in China. Halophytes can effectively improve salt-affected soils through salt-removing processes, such as salt exclusion and excretion [12]. However, most of the halophyte biomass is not properly utilized. These biomass wastes are conventionally treated via landfill disposal or incineration, leading to extra environmental pollution [14]. Halophytes are valuable biomass resources rich in cellulose and lignin, which can be utilized for biochar preparation [13, 15, 16]. The type of biomass, activating agents, and modification methods have a significant influence on biochar properties [17]. Phosphoric acid (H_3PO_4) and pyrophosphoric acid ($H_4P_2O_7$) are common activators. They have been widely applied for the functionalization of biomass [18, 19]. Previous studies reported that biochar prepared by $H_4P_2O_7$ activation biomass had more total acidic groups and a lower pH value (5.76) than that after H_3PO_4 activation treatment, because $H_4P_2O_7$ is more acidic than H_3PO_4 [5, 19, 20]. Nevertheless, the potential of H_3PO_4- and $H_4P_2O_7$-modified biochar as alkaline soil amendments for P activation and improved soil properties remains unknown.

This study involved the hypothesis that H_3PO_4 and $H_4P_2O_7$ modification improves structural characteristics and that the P-binding form in HBC, and P-rich biochar facilitates the activation of P in alkaline soils. The main objectives of this study were to (1) investigate the basic properties of H_3PO_4- and $H_4P_2O_7$-modified halophyte biochar, (2) qualitatively and quantitatively study the combination mode and fractions of P in P-HBC and PA-HBC, and (3) explore the influences of P-rich biochar on the soil P fractions and transformation.

Materials and methods

Soil and chemical reagents

Surface alkaline soil samples (0 to 20 cm) were collected from fallow fields at research farms: aeolian sandy soils (AS) were collected from the Soil Improvement Test Station, Xinjiang (86° 24′ E, 45° 20′ N), gray desert soils (GS) were collected from the Experiment Station of Xinjiang Academy of Agricultural Sciences, Qitai (89° 12′ E, 44° 13′ N), brown desert soils (BS) and saline soils (SS) were collected from the National Field Scientific Observation and Research Station of Farmland Ecosystem, Aksu (80° 45′ E, 40° 37′ N). The basic properties of the soils are shown in Additional file 1: Table S1. Ultrapure water (18.2 M' Ω cm, Millipore, USA) was used to prepare the desired solution. All the chemicals and reagents used in the present study were of analytical grade.

Biochar production and characterization

The biomass precursor was Salicornia angustifolia (*Salicornia europaea* L.). The halophytes were air-dried at 60 °C, washed with de-ionized water to remove dust and impurities, placed in a quartz reactor and then heated at 15 °C·min^{-1} in a muffle furnace in a N_2 environment at 400 °C for 2 h (hereafter referred to as HBC). After pyrolysis, the HBC was homogenized and ground through a 50-mesh sieve. H_3PO_4-modified biochar (P-HBC) and $H_4P_2O_7$-modified biochar (PA-HBC) were obtained by impregnating HBC with H_3PO_4 solution (70 wt.%) and $H_4P_2O_7$ at a ratio of 20:1 (solution/g HBC). $H_4P_2O_7$ was obtained by the dehydration of phosphoric acid at 213 °C. Mixed samples were shaken continuously for 24 h at 120 rpm on an orbital shaker. After modification, the samples were washed with distilled water until the pH of the washed solution was constant.

The suspensions were shaken for 30 min at 150 rpm, the pH and electrical conductivity (EC) were determined at a solid:water ratio of 1:5 (w/v) using a pH meter (FE20 plus, Mettler Toledo, Switzerland) and an EC meter (BEC-6500A, Bell, America). The element compositions of the biochar were determined using an elemental analyzer (EA3000, Jena, Germany). The surface morphology was examined by field emission scanning electron microscopy–energy dispersive spectroscopy (SEM–EDS) (S-4800, Hitachi, Japan). The specific surface area was determined by the sorption of N_2 at 77 K using a BELSORP-MAX analyzer and calculated using the Brunauer Emmett teller (BET) equation. Fourier transform infrared spectroscopy (FTIR) was performed on HBC before and after modification with an FTIR-4100 spectrometer (Jasco, Japan). The HBC sample and spectroscopy grade KBr were dried at 105 ℃ for 4 h, and then the sample was coground with KBr (1:100, wt/wt). The mixture was pressed into a pellet under infrared lamp exposure. The spectra were collected in the range of 4000 to 400 cm^{-1} at a step of 4 cm^{-1}. X-ray photoemission spectroscopy (XPS) measurements were carried out using the Thermo Fisher ESCALAB 250Xi system. The photoelectrons were excited by Al-Kα radiation ($h\nu = 1486.8$ eV). The binding energy was scanned from 1200 to 0 eV. The full element spectrum and the survey scans of the C 1s, O 1s and P 2p spectra were analyzed. The XPS data were processed using XPSPEAK41 software. The contents of elements were evaluated from the ratios of the areas under the corresponding core-level peaks of the survey spectra.

Soil incubation experiments

Before starting the experiment, the soil samples were air-dried and sieved through a 2-mm standard sieve. One hundred grams of air-dried soil sample was weighed and placed into a 500 mL plastic culture bottle (12.8 cm depth, 7.9 cm diameter). Then, the four types of soil (AS, BS, GS and SS) were mixed with HBC, P-HBC and PA-HBC at ratios of 0 (control) and 1%.

The incubation experiment included 16 treatments (including the control), each bottle was regarded as a replicate, and 4 replicates (bottles) were used for each treatment. A total of 64 bottles were incubated at 25 °C for 60 d in an incubator. The de-ionized water was added every 2–3 days on a weight basis to maintain the targeted water content (60% of water holding capacity). Plastic films with 10 small holes were applied to cover the tops of the bottles to ventilate and reduce moisture losses. When the incubation was completed, the mixed samples were air-dried and sieved (100 mesh) for later analysis.

Determination of chemical properties

Soil pH and EC were analyzed from 1:5 soil–water extracts using the probes of a FE20 plus pH meter and BEC-6500A conductivity meter. Soil organic matter was measured using the external-heat potassium dichromate oxidation and titration method. The soil soluble sodium (Na^+) and potassium (K^+) contents were estimated with flame photometry (FP6410, Jingke Analytical Instruments, China). The soluble calcium (Ca^{2+}) and magnesium (Mg^{2+}) contents of the soil samples were determined by atomic absorption spectrometry (RG3604, Hirp, China).

The P fractions in each treatment were analyzed through a sequential extraction process [21]. Briefly, 0.5 g of sample was placed in a 50 mL centrifuge tube and extracted with 30 mL of H_2O for 1 h and then sequentially with 0.5 M $NaHCO_3$ at pH 8.5 (16 h), 0.1 M NaOH at pH 13 (16 h), and 1.0 M HCl (16 h). After every addition of extractant, the samples were centrifuged on an orbital shaker at 4000 rpm for 15 min. The total P (P_t) content in

biochar extracts was measured by digesting the extracts in a microwave at 140 °C for 60 min. Inorganic P (P_i) was analyzed by direct extraction. The organic P (P_o) was the difference between Pt and Pi in extracts of $NaHCO_3$ and NaOH. Then, the residue from HCl extraction was dissolved with 10 mL of H_2SO_4·H_2O_2 and digested in a microwave at 300 °C for 2 h. Absorbance was measured at 880 nm using the molybdate–ascorbic acid method with a spectrophotometer (Spectrumlab 22pc, LASPEC, China) to analyze P.

Statistical analyses

All experiments were conducted in quadruplicate. Experimental data are listed as the means ± standard deviations. One-way analysis of variance was carried out using SPSS 20.0. Origin Pro 2021 software was used for graphing. Multiple comparisons were made by the least significant difference test ($p < 0.05$). Pearson's correlation analysis with a significance level of $p < 0.05$ and $p < 0.01$ was used to quantify the correlation between variables.

Results

Characterization of biochars

The element compositions and BET of the biochars are listed in Table 1. Compared with the HBC, the C content decreased significantly by 14.17% and 27.34%, while the O content increased by 11.83% and 27.93% in the P-HBC and PA-HBC samples, respectively. The O/C and H/C ratios of P-HBC and PA-HBC increased relative to those of HBC. The ash content was significantly increased in P-HBC and PA-HBC relative to that in HBC. Moreover, the surface area and pore volume of biochar followed the order of PA-HBC (0.71 $m^2 \cdot g^{-1}$) < P-HBC (1.00 $m^2 \cdot g^{-1}$) < HBC (11.89 $m^2 \cdot g^{-1}$). The three biochars were mainly mesoporous (2–50 nm). The average pore diameters of HBC, P-HBC, and PA-HBC were 7.17 nm, 3.78 nm, and 2.43 nm, respectively.

Textural structure analysis of biochars

The pore size distribution and N_2 adsorption–desorption isotherms at 77 K of the biochars are shown in Fig. 1. HBC exhibited a typical Type IV adsorption isotherm, indicating a mesoporous structure for HBC. The adsorption–desorption isotherms of P-HBC and PA-HBC presented Type I curves, which suggested that P-HBC and PA-HBC possessed narrow pore size distributions in the micropore range.

The differences in the surface morphology and P distribution of HBC before and after modification were observed through SEM–EDS imaging (Fig. 2). A granular structure with a high P content was formed on the surface of the modified biochar. The P contents on the surfaces of P-HBC and PA-HBC were significantly increased compared to that on the surface of HBC by 9.16% and 11.55%, respectively (Additional file 1: Table S2).

Table 1 Element compositions and BET of halophyte biochar (HBC), H_3PO_4-modified biochar (P-HBC), and $H_4P_2O_7$-modified biochar (PA-HBC)

Property	Treatment		
	HBC	P-HBC	PA-HBC
C (%)	59.79	45.62	32.45
N (%)	1.07	0.56	0.84
H (%)	2.96	3.13	1.85
O (%)	11.81	23.64	39.74
Atomic ratio O/C	0.15	0.39	0.92
Atomic ratio H/C	0.59	0.82	0.68
Ash (%)	24.37	27.06	26.12
BET surface area ($m^2 \cdot g^{-1}$)	11.89	1.00	0.71
Average pore diameter (nm)	7.17	3.78	2.43
Total pore volume ($cm^3 \cdot g^{-1}$)	0.0291	0.0010	0.0007

O% = 100%–(C% + N% + H% + Ash%)

Chemical properties and P morphology analysis of biochar

The existence of functional groups of P in all samples was investigated via FTIR spectroscopy within a scanning range of 4000–400 cm^{-1} (Fig. 3). The multiple signals were superpositioned at 2416, 1420, 1085, 799 and 490 cm^{-1}. After modification, the absorption peak intensity of the biochar was observed to increase significantly at 490 cm^{-1}, proving that the modification process can effectively promote the formation and stabilization of the P–$(OH)_3$ bond. The peak of C–P stretching at 799 cm^{-1} disappeared, as previously reported [22], indicating that H_3PO_4 and $H_4P_2O_7$ destroyed the P–C present in the original biochar. Within this range, the peak at 1085 cm^{-1} can be attributed to the ionized P–O linkage and the symmetrical vibration of P–O–P in polyphosphate chains [23]. The peaks in the region of 1420 cm^{-1} were assigned to the carboxylic (−COOH) stretching vibration. P-HBC and PA-HBC exhibited new absorption peaks at 2416 cm^{-1}, which were attributed to PH_3 or P–H.

The HBC samples were alkaline with a pH of 10.18. After being modified by H_3PO_4 and $H_4P_2O_7$, the pH of HBC was reduced significantly, and the pH values of P-HBC and PA-HBC were 3.31 and 2.17, respectively (Fig. 4a). The EC of HBC was 3.35 $ds \cdot m^{-1}$, which was not significantly different from those of P-HBC and PA-HBC (Fig. 4b). The total P of the modified samples increased significantly in the order of HBC (0.51 $g \cdot kg^{-1}$) < P-HBC (4.66 $g \cdot kg^{-1}$) < PA-HBC (5.24 $g \cdot kg^{-1}$) (Fig. 4c). The proportions occupied by the P fractions in each treatment are presented in Fig. 4d. In particular, P-HBC and

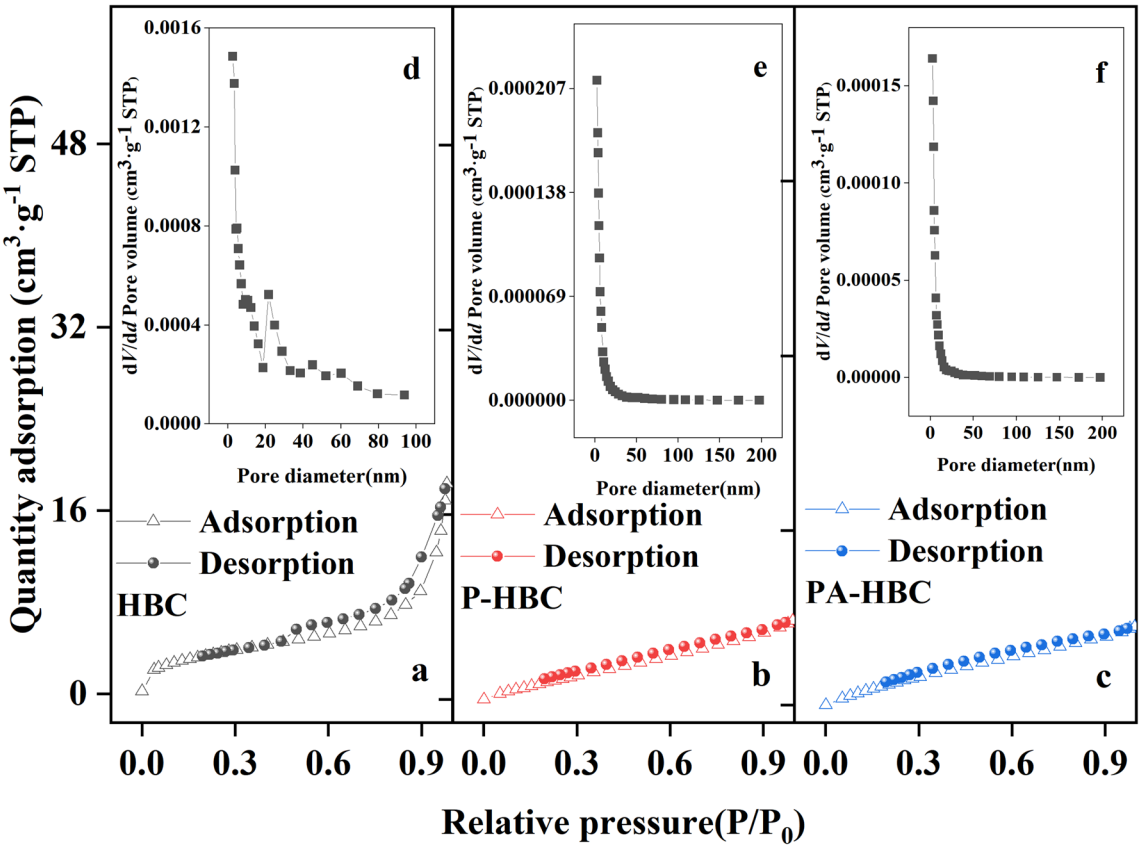

Fig. 1 N_2 adsorption–desorption isotherms (**a**–**c**) and pore size distribution (**d**–**f**) of HBC, H_3PO_4-modified biochar (P-HBC), and $H_4P_2O_7$-modified biochar (PA-HBC)

PA-HBC had proportions of H_2O-extractable P that were increased by 70.10% and 61.60% in biochars, respectively, compared to the HBC. The concentration of HCl-P decreased by 30.16% and 30.25% in P-HBC and PA-HBC, respectively, in contrast to the HBC. Furthermore, the concentration of Rs-P decreased by 32.12% and 30.40%, respectively.

The chemical composition and bonding configurations of P on the biochar were further analyzed by XPS, and the results are presented in Fig. 4e. Three characteristic peaks appeared at approximately 132 eV, 286 eV, and 534 eV corresponding to the P 2p, C 1s, and O 1s peaks in the samples (P-HBC and PA-HBC). In particular, the P 2p peak was not observed for HBC, further illustrating the successful loading of P atoms into the modified samples. With the help of XPS analysis, the C, O and P on the surface of the modified samples were semiquantitatively estimated (Additional file 1: Table S3). After modification, the percent C content tended to decrease. The data also indicate that the values of O increased after modification.

To further understand the chemical bond configuration of P in the activated biochar, the high-resolution P 2p and O 1s peaks of both P-HBC and PA-HBC were deconvoluted, and the components were semiquantitatively analyzed to obtain their peak areas, as shown in Fig. 4f, g and Additional file 1: Table S4. Three major peaks at approximately 133.1 eV (C–P–O), 134.0 eV (C–O–P), and 135.0 eV (O=P–O) appeared for the P 2p peaks of both P-HBC and PA-HBC, of which the peak at 135.0 eV was assigned to pyrophosphate [24]. The O 1 s spectra of P-HBC and PA-HBC were deconvoluted into three peaks assigned to C=O and/or P=O (approximately 531.0 eV), P–O–C and/or C–O–C (approximately 532.2 eV), and P–O–P (approximately 533.5 eV) [25]. Compared with P-HBC, the percent C–O–P of PA-HBC increased from 34.79% to 37.24% (Additional file 1: Table S4). After modification, the deconvolution results of the O 1 s peaks showed an increase in the proportion of P–O–C and/or C–O–C from 35.40% to 43.91% and 42.10%, as well as an increase in the proportion of P–O–P from 4.94 to 24.05% and 22.61%, respectively (Additional file 1: Table S4). The binding energy of C=O and/or P=O, as well as C–O–C and/or P–O–C bonding, shifted positively with P doping, inducing a high binding energy. Overall, P was mainly

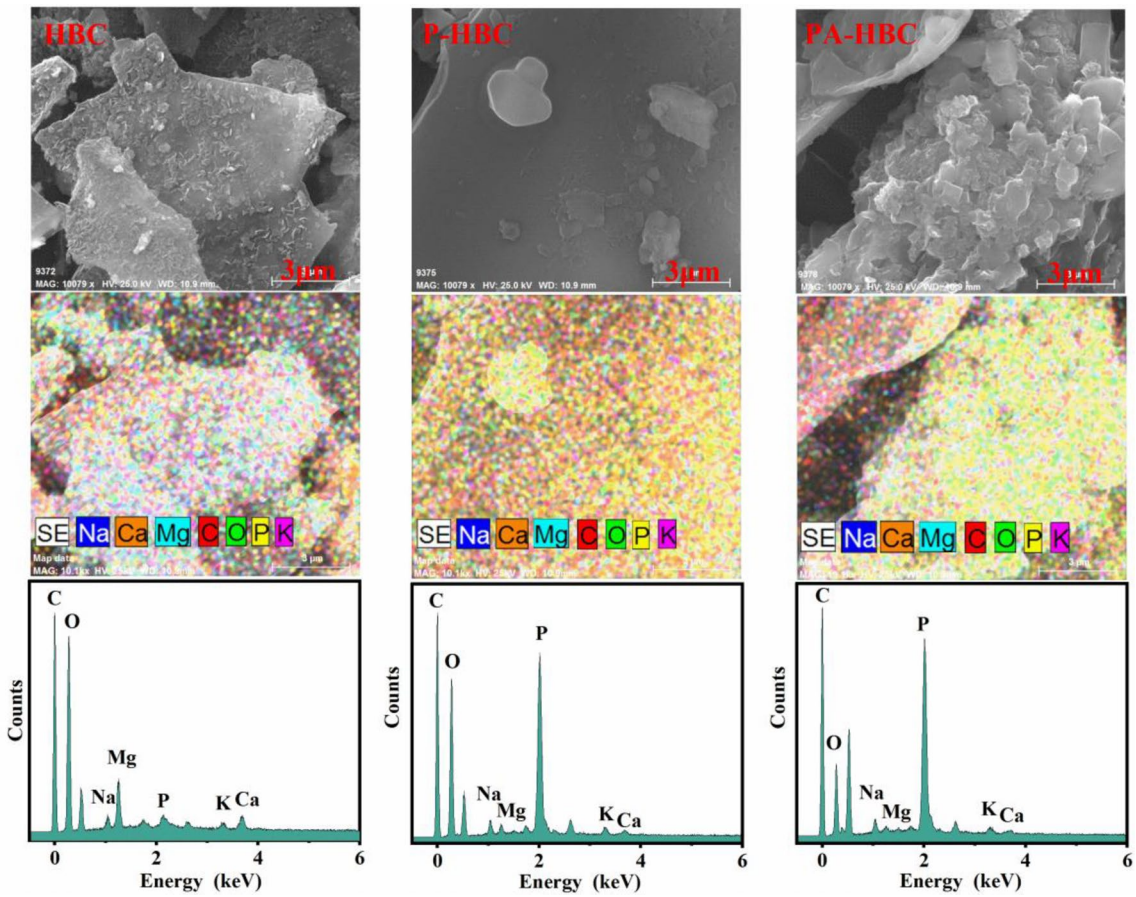

Fig. 2 Scanning electron microscopy energy dispersive spectroscopy (SEM–EDS) imaging of the halophyte biochar (HBC), H_3PO_4-modified biochar (P-HBC), and $H_4P_2O_7$-modified biochar (PA-HBC)

bound on the surface of biochar by directly bonding with C atoms or bridged by O atoms.

Effects of biochars on soil

The pH, EC and total P of the soil differed depending on the type of biochar that was added (Fig. 5). The soil pH values of both P-HBC-treated and PA-HBC-treated were significantly reduced to 7.16–7.45. The addition of HBC increased the EC values of BS and GS to 5.13 $ds{\cdot}m^{-1}$ and 1.50 $ds{\cdot}m^{-1}$, respectively. The application of biochar showed an insignificant impact on the total P in the soils. The addition of modified biochars with quite low pH values in alkaline soils tended to change the soil pH to neutral, which had a positive impact on seed germination and plant growth. In contrast, the original biochar increased the EC values of some soil types to excessively high levels.

Figure 6 shows the results of the sequential extraction of the different soils after 60 days of incubation. The effect of HBC on the soil P fractions depended on the type of alkaline soils. After the application of HBC, organic P ($NaHCO_3$–Po and NaOH–Po) increased by 4.19–10.96% in AS and BS. Inorganic P ($NaHCO_3$–Pi and NaOH–Pi) was decreased in GS and increased in SS. Regardless of the status of the P fractions of the control experimental soils (CK), H_2O–P increased significantly in soils (2.13–26.02%) with the application of P-HBC and PA-HBC to alkaline soils. The application of the modified biochar (P-HBC and PA-HBC) increased the inorganic P ($NaHCO_3$–Pi and NaOH–Pi) content by 1.28–29.01%. In addition, the concentration of organic P ($NaHCO_3$–Po and NaOH–Po) was reduced by 0.40–20.45% in modified biochar-treated soils. It must be mentioned that the HCl–P content only increased in SS compared to the control. The biochars in the soils enhanced the transformation ability of Rs–P. The Rs–P decreased by 2.35–40.62% due to biochar application. This phenomenon was weaker in the HBC treatment and stronger in the P-HBC treatment and PA-HBC treatment.

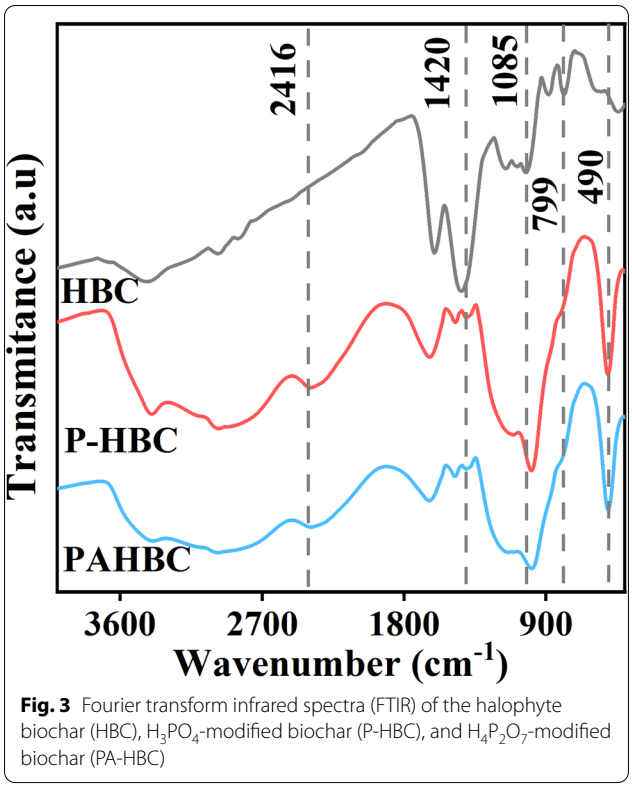

Fig. 3 Fourier transform infrared spectra (FTIR) of the halophyte biochar (HBC), H_3PO_4-modified biochar (P-HBC), and $H_4P_2O_7$-modified biochar (PA-HBC)

In correlating the P fractions of biochars versus the soil characteristics, it was observed that the interactions between these factors changed completely depending on the different analyzed alkaline soil types (Fig. 7). The contents of H_2O–P and Rs–P in the biochars were negatively correlated with soil pH in all alkaline soil treatments. The inorganic P ($NaHCO_3$–Pi and NaOH–Pi) in the biochars had negative relationships with the organic P ($NaHCO_3$–Po and NaOH–Po) in the soils, respectively. The inorganic P ($NaHCO_3$–Pi and NaOH–Pi) and Rs–P in the biochars had negative correlations with soil pH. In addition, it was observed only in SS that biochar NaOH–Po was positively correlated with soil HCl–P, whereas it was negatively correlated with soil Rs–P. Finally, it was found that biochars can change the availability of P by transforming P fractions through changes in soil properties.

Discussion

The properties of biochars are known to exhibit deviation over a wide range due to differences in modified and unmodified materials (here, H_3PO_4 and $H_4P_2O_7$). The O/C atomic ratio in HBC was < 0.2, suggesting a longer stability and half-life of HBC [28]. Halophytes are rich with cations, such as Ca, K, Mg, and Na [13, 14]. After pyrolysis, these cations form carbonates and oxides, increasing the pH of HBC [15, 27]. Both H_3PO_4 and $H_4P_2O_7$ are oxygen-rich phosphoric acids that easily react with the soluble minerals of halophytes, forming insoluble phosphate salts [29]. Due to the formation and accumulation of mineral elements in the modified biochars, the ash content increased significantly. The pores of the biochar were blocked by phosphate salts, resulting in a decrease in pore volume, which corroborated the findings of Liu et al. [31]. The spectral and elemental analysis showed that the values of O increased after modification, which could be attributed to the formation of −COOH and oxygen-containing phosphate groups after modification by oxygen-rich acid [15]. The formation of these acid groups was the primary reason for the changes in the chemical properties of biochars. The results revealed that fresh P-containing and acidic functional groups were formed in P-HBC and PA-HBC, which are essential for application in alkaline soils. Furthermore, the C content of biochar decreased after H_3PO_4 and $H_4P_2O_7$ modification. This may be due to the instability of the edge of the biochar, whereby C is easily replaced by O or P or is lost in the form of CO or CO_2 generated by the reaction of biochar with acid [26]. $H_4P_2O_7$ has a higher acidity and more oxygen content than H_3PO_4. Therefore, the content of O atoms with a higher electronegativity increased owing to the partial oxidization of biochar by $H_4P_2O_7$ [26]. This facilitated the formation of more C–O–P in PA-HBC. The positively shifted binding energy of the O 1s peak have occurred, because charge was transferred from the C atom to the P atom, thus forming a chemical bond with P in P-HBC and PA-HBC [26]. We observed that more oxidized P was covalently bonded with C in PA-HBC than in P–HBC. Based on molecular orbital calculations, the O–P bond was found to be the weakest, and the C–P bond may be more stable than the C–O–P bond [25]. Through modification by H_3PO_4 and $H_4P_2O_7$, the association of P with C bridged by O in biochars increased, and it was the highest in PA-HBC. Therefore, the effectiveness of P might be relatively high in PA-HBC, followed by P-HBC. This conjecture was proven by the sequential extraction of P.

The sequential fraction method considers that the effectiveness of the extraction of P species gradually decreases in the order of water, $NaHCO_3$, NaOH, and HCl, and the remaining P in the residue is considered to be the least effective form [30]. The pyrolysis process of biochars can lead to the conversion of P into more recalcitrant forms. As a result, higher proportions of HCL–P and Rs–P accumulate in HBC [5, 32]. Adhikari et al. [33] reported a high proportion of HCL–P (57.60%) in biochar prepared at 400 ℃. However, in this study, the proportion of HCL–P (33.43%) was similar to Rs–P (39.29%), which could be attributed to the high levels of mineral components in halophytes [15]. HCl–P and Rs–P represent occluded P, with a slow

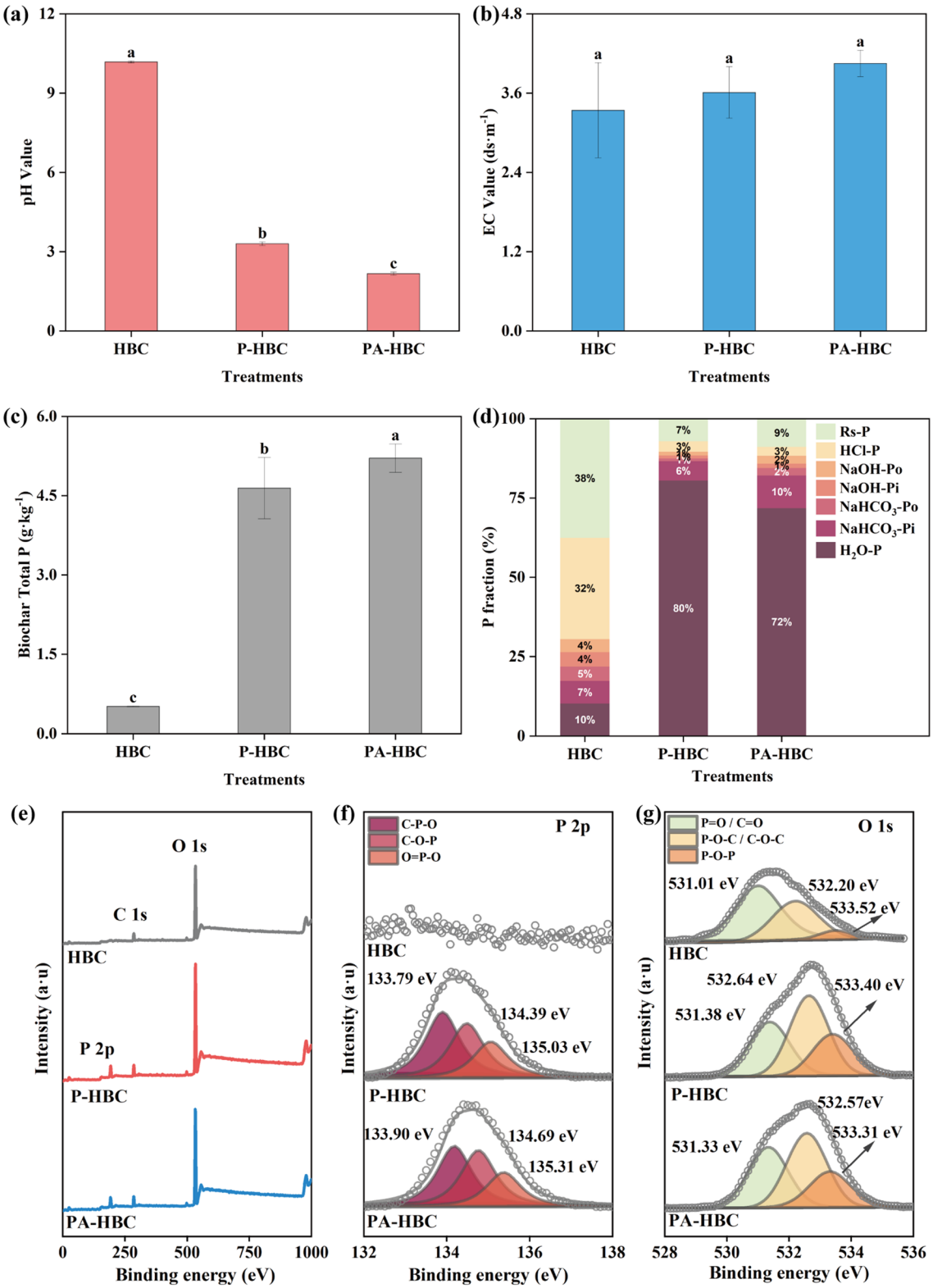

Fig. 4 Influence of H_3PO_4 and $H_4P_2O_7$ modified on pH (**a**), electrical conductivity (EC) (**b**), total P (**c**), and relative proportion of each P fractions in the biochars (d); X-ray photoelectron spectroscopy (XPS) spectrum of the halophyte biochar (HBC), H_3PO_4-modified biochar (P-HBC), and $H_4P_2O_7$-modified biochar (PA-HBC) (**e**); high-resolution XPS spectrum of P2p (**f**); and high-resolution XPS spectrum of O1s (**g**). Error bars are standard deviation of the means ($n = 4$). Different letters above the bars indicate significant ($p < 0.05$) difference between treatments

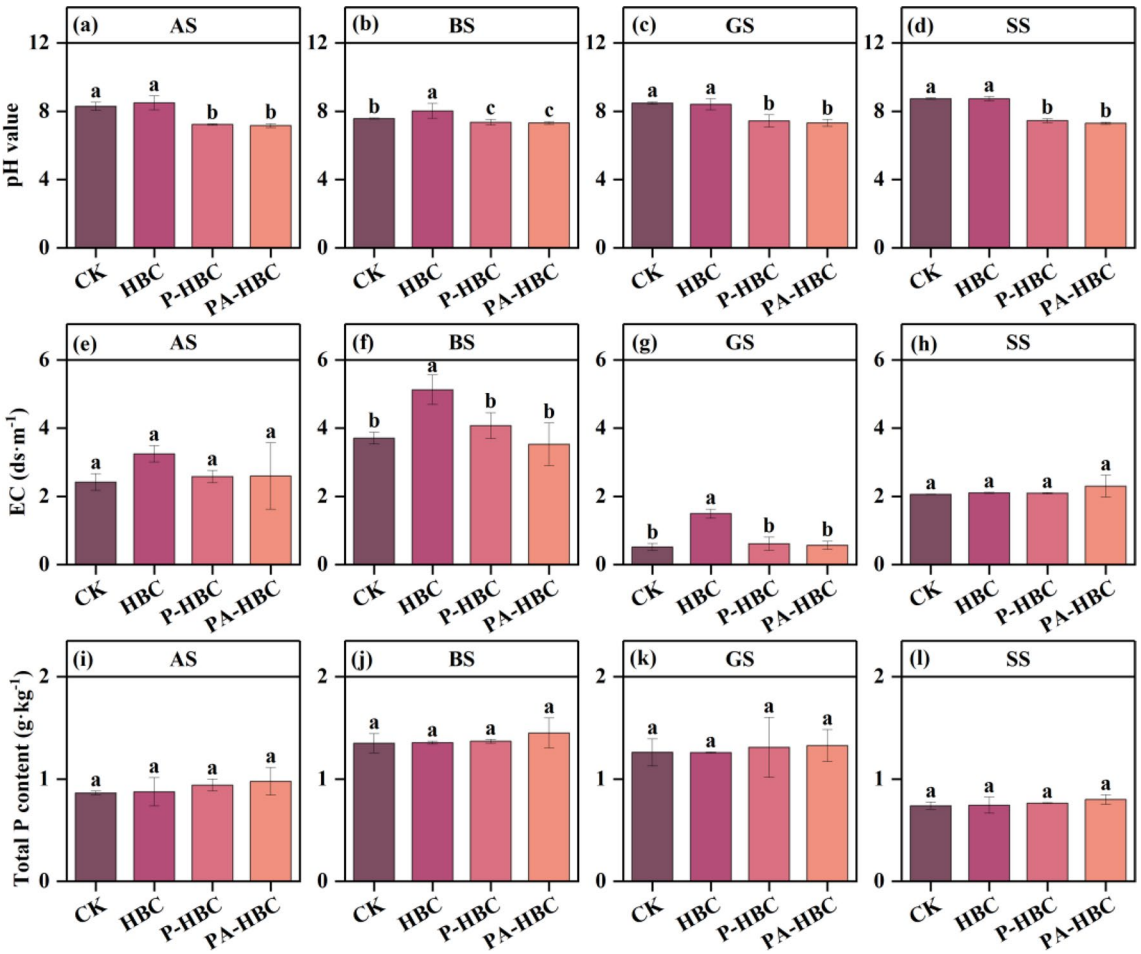

Fig. 5 Influence of halophyte biochar (HBC), H_3PO_4-modified biochar (P-HBC), and $H_4P_2O_7$-modified biochar (PA-HBC) on pH (**a**–**d**), electrical conductivity (EC) (**e**–**h**) and total P (**i**–**l**) in the soils. Control: untreated soil (CK); AS: aeolian sandy soils; BS: brown desert soils; GS: grey desert soils; SS: saline soils. Error bars are standard deviation of the means ($n = 4$). Different letters above the bars indicate significant ($p < 0.05$) difference between treatments

turnover and consisting of P bound to calcium (Ca) and other cations [33]. The pH also showed a positive correlation with the Rs–P fraction, indicating that high pH is related to high amounts of Rs–P [21]. HBC was rich in cations, such as Ca and magnesium (Mg), and had a high pH value (10.24), which promoted the formation of HCl–P and Rs–P in HBC. Compared with HBC, the content of HCl–P was reduced after modification. This discrepancy might be because HCl–P transformed into other forms of P. Acidic groups such as −COOH and phosphoric acid groups on the surface of the biochar were enriched by H_3PO_4 and $H_4P_2O_7$ modification. In an acidic environment, the −COOH groups react with Ca and Mg to inhibit the formation of insoluble P forms. While the desorption of P in the original biochar occurred due to the addition of acid, it resulted in a reduced HCl–P fraction [34].

The availability of P is mainly affected by pH and metal oxide adsorption in the soil. Along with HBC, the metal cations in biochar also entered the soil. A high pH value increases the precipitation of P to make the forms of P stable. In alkaline soils and HBC, there are a large number of free cation oxides that could be sites for P sorption [5, 12, 35]. This may have led to the increase in the organic P ($NaHCO_3$_Po and NaOH–Po) content in the soil after HBC application. After the application of modified biochars with acidity, the alkaline soils tended to be neutral due to the high buffering capacity of soils. The organic P fraction ($NaHCO_3$_Po and NaOH–Po) in the soil was transformed after the application of P-HBC and PA-HBC. This is because the organic acids bound in the modified biochars can provide organic anions, the bonds between organic anions and cations are stronger than those between phosphates and

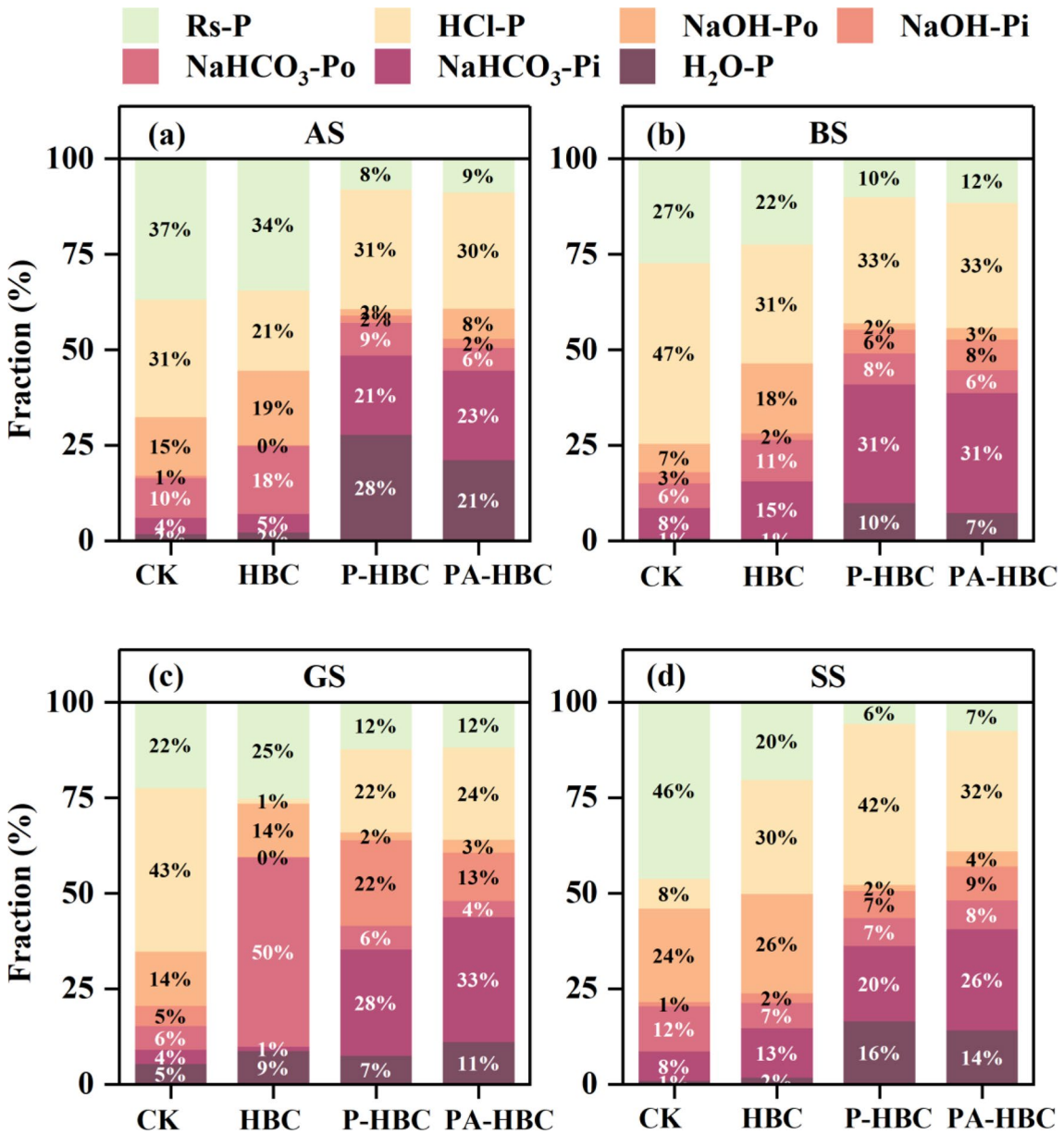

Fig. 6 Influence of halophyte biochar (HBC), H_3PO_4-modified biochar (P-HBC), and $H_4P_2O_7$-modified biochar (PA-HBC) on relative proportion of each P fractions in the AS **a**, BS **b**, GS **c** and SS **d**. Control: untreated soil (CK); AS: aeolian sandy soils; BS: brown desert soils; GS: grey desert soils; SS: saline soils

cations [34, 36, 37]. The change in P fractions was also affected by several processes, such as the adsorption of P to cations and metal oxides, mineralization, dissolution, and precipitation to mineral pools. The application of P-HBC and PA-HBC reduced the pH of the soil, thus causing an increase in the amount of free cation oxides in the soil compared with that in biochar. The application of acidic biochars can greatly increase the available P fraction (H_2O–P and $NaHCO_3$_Pi) content in alkaline soil due to competition of free cations in the soil for phosphate adsorption sites [11, 38]. Therefore, when incorporated into the soil, modified biochars can change the availability of P by indirectly transforming P fractions through changes in soil properties, as suggested by Glaser et al. [7] and Figueiredo et al. [39].

The effects of biochars on diverse alkaline soils were also different. Compared to that in the other soils, the greater amount of metal cations in SS provided more substrates for the reaction, although AS, BS and GS also contained cations. The increased concentrations

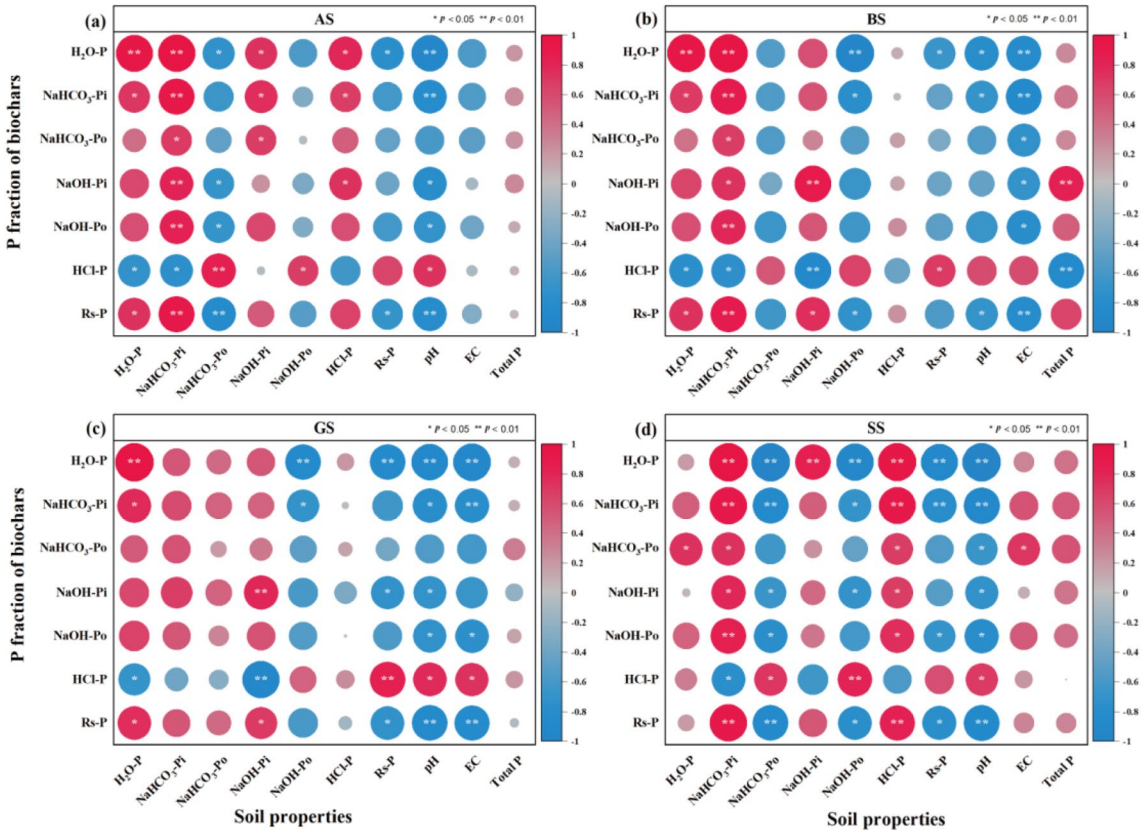

Fig. 7 Pearson correlation matrix featuring relationships between soil properties and biochar P fractions. AS: aeolian sandy soils **a**; BS: brown desert soils **b**; GS: grey desert soils **c**; SS: saline soils **d**. Correlation significance was set at $*p < 0.05$, $**p < 0.01$

of HCl–P only observed for the SS treatments might be ascribed to the sorption/precipitation of P with the excess of cations in SS [21]. Furthermore, a significant correlation between stable P forms (HCl–P and Rs–P) and NaOH–Po was noted only for SS, which may have occurred for two reasons: (i) the dissolved organic matter released from biochar in the form of organic ligands can form organometals. SS contained a greater metal-ion content than the other soils, and the response of Rs–P to organic P fractions was more obvious and thus increased the Rs–P transformation rate related to NaOH–Po [40]. (ii) The excess of metal ions in SS can form HCl–P in soil due to mineralization between organic P and cations, and thus, the HCl–P in SS was strongly controlled by factors, such as organic P fractions ($NaHCO_3$–Po and NaOH–Po) [41].

Conclusions

In conclusion, these results indicate that H_3PO_4 and $H_4P_2O_7$ modifications are a feasible option for enhancing the sustainable use of P in alkaline soils. The H_3PO_4 and $H_4P_2O_7$ modifications were effective for decreasing the pH value, specific surface area, and pore volume. Although C was partially lost in the process of modification, mineral nutrients (especially P) were concentrated in the biochars. The spectral characterization revealed that the association of P directly with C or indirectly with C through O increased the P content in biochar. P-HBC and PA-HBC had higher total P and active P than HBC, while HBC was high in HCl–P and Rs–P. In addition, biochar enhanced the available concentration of P in the soil by improving the soil properties and transformed soil P fractions. In particular, the modified biochar was found to be more efficient in increasing available P fractions than the original biochar. In summary, P-rich biochar could be an effective candidate for positively impacting alkaline soil properties and P availability.

Abbreviations

HBC: Halophyte biochar; P-HBC: H_3PO_4-modified biochar; PA-HBC: $H_4P_2O_7$-modified biochar; AS: Aeolian sandy soils; BS: Brown desert soils; GS: Gray desert soils; SS: Saline soils; CK: Untreated soil.

Supplementary Information

The online version contains supplementary material available at https://doi.org/10.1186/s40538-022-00374-4.

Additional file 1: Table S1. General physical and chemical properties of the soil. **Table S2.** Element analysis of the halophyte biochar (HBC), H_3PO_4-modified biochar (P-HBC), and $H_4P_2O_7$-modified biochar (PA-HBC) by scanning electron microscopy energy dispersive spectroscopy (SEM–EDS). **Table S3.** Element analysis of the halophyte biochar (HBC), H_3PO_4-modified biochar (P-HBC), and $H_4P_2O_7$-modified biochar (PA-HBC) by X-ray photoelectron spectroscopy (XPS). **Table S4.** Relative content of phosphorus species of the P2p and O1s peaks of halophyte biochar (HBC), H_3PO_4-modified biochar (P-HBC), and $H_4P_2O_7$-modified biochar (PA-HBC).

Acknowledgements
Not applicable.

Author contributions
XW, TS and GT conceived and designed the study, and wrote the manuscript. GT, MA, HM, MC, GY, and HJ were responsible for performing the field and laboratory work. XW and HJ analyzed the data. All authors discussed the results, critically reviewed the manuscript, and approved its publication. All authors read and approved the final manuscript.

Funding
This research was supported by the National Natural Science Foundation of China (31660073) and National Key Research and Development Program of China (2018YFD0200406).

Availability of data and materials
All data generated or analyzed during this study are included in this published article.

Declarations

Ethics approval and consent to participate
Not applicable.

Consent for publication
Not applicable.

Competing interests
The authors declare that there are no conflicts of interest to declare.

Author details
[1]College of Resources and Environment Sciences, Xinjiang Agricultural University, East Nongda Road No. 311, Urumqi 830052, China. [2]Key Laboratory of Original Environmental Pollution Prevention and Control, Ministry of Agriculture and Rural Affairs/Tianjin Key Laboratory of Agro-Environment and Agro-Products, Agro-Environmental Protection Institute, Ministry of Agriculture and Rural Affairs, Tianjin 300191, China. [3]Institute of Soil and Fertilizer & Agricultural Sparing Water, Xinjiang Academy of Agricultural Science, Urumqi 830091, China. [4]College of Grassland Science, Xinjiang Agricultural University, Urumqi 830052, China.

Received: 6 October 2022 Accepted: 14 December 2022
Published online: 27 December 2022

References

1. Duan ML, Liu GH, Zhou BB, Chen XP, Wang QJ, Zhu HY, Li Z. Effects of modified biochar on water and salt distribution and water-stable macro-aggregates in saline-alkaline soil. J Soils Sediments. 2021;21(6):2192–2202.
2. Elkhlifi Z, Kamran M, Maqbool A, El-Naggar A, Ifthikar J, Parveen A. Phosphate-lanthanum coated sewage sludge biochar improved the soil properties and growth of ryegrass in an alkaline soil. Ecotoxicol Environ Saf. 2021;216(15):112–173.
3. Seoud AEIIIA. Effect of biochar rates on A-mycorrhizal fungi performance and maize plant growth, Phosphorus uptake, and soil P availability under calcareous soil conditions. Commun Soil Sci Plant Anal. 2021;52(8):815–831.
4. Zhang H, Zhang J, Zhang F, Liu D, Wei C. Effects of different phosphorus fertilizerson soil phosphorus availability and maize yield under drip irrigation. J Soil Water Conserv. 2019;33 (02): 189-195.
5. Xu G, Zhang Y, Shao HB, Sun JN. Pyrolysis temperature affects phosphorus transformation in biochar: chemical fractionation and ^{31}P NMR analysis. Sci Total Environ. 2016;569:65–72.
6. Kizito S, Luo HZ, Lu JX, Bah H, Dong R, Wu S. Role of nutrient-enriched biochar as a soil amendment during maize growth: exploring practical alternatives to recycle agricultural residuals and to rreduce chemical fertilizer demand. Sustainability. 2019;11:11–32.
7. Glaser B, Lehr VI. Biochar effects on phosphorus availability in agricultural soils: a meta-analysis. Sci Rep. 2019; 9: 3269–3282.
8. Chen M, Nurguzal A, Zhang YT, Xu N, Cao XD. Contrasting effects of biochar nanoparticles on the retention and transport of phosphorus in acidic and alkaline soils. Environ Pollut. 2018;239:562–570.
9. Qian TT, Zhang XS, Hu JY, Jiang H. Effects of environmental conditions on the release of phosphorus from biochar. Chemosphere. 2013;9(93):69–75.
10. Mukherjee S, Mavi MS, Singh J, Singh BP. Rice-residue biochar influences phosphorus availability in soil with contrasting P status. Arch Agron Soil Sci. 2019;66(7):778–791.
11. Kamran MA, Xu RK, Li JY, Jiang J, Shi RY. Impacts of chicken manure and peat-derived biochars and inorganic P alone or in combination on phosphorus fractionation and maize growth in an acidic ultisol. Biochar. 2019;1(3):283–291.
12. Rozentsvet OA, Nesterov VN, Kosobryukhov AA, Bogdanova ES, Rozenberg GS. Physiological and biochemical determinants of halophyte adaptive strategies. Russ J Ecol. 2021;52:27–35.
13. Hasanuzzaman M, Nahar K, Alam MM, Bhowmik PC, Hossain MA, Raham MM, Prasad MNV, Ozturk M, Fujita M. Potential use of halophytes to remediate saline soils. Biomed Res Int. 2014;12:1–9.
14. Xiao H, Lin Q, Li G, Zhao X, Li J, Li E. Comparison of biochar properties from 5 kinds of halophyte produced by slow pyrolysis at 500 °C. Biochar. 2022;4(12):2–10.
15. Wei J, Tu C, Yuan G, Liu Y, Bi D, Xiao L, Lu J, Theng BKG, Wang H, Zhang L, Zhang H. Assessing the effect of pyrolysis temperature on the molecular properties and copper sorption capacity of a halophyte biochar. Environ Pollut. 2019;251:56–65.
16. Marzooqi AF, Yousef LF. Biological response of a sandy soil treated with biochar derived from a halophyte (*Salicornia bigelovii*). Appl Soil Ecol. 2017;114:9–15.
17. Gao Y, Yue QY, Gao BY. Insights into properties of activated carbons prepared from different raw precursors by pyrophosphoric acid activation. J Environ Sci. 2016;41:235–243.
18. Sun YY, Yue QY, Gao BY, Wang Y, Gao Y, Li Q. Preparation of highly developed mesoporous activated carbon by $H_4P_2O_7$ activation and its adsorption behavior for oxytetracycline. Powder Technol. 2013;249:54–62.
19. Cheng C, Zhang J, Mu Y, Gao JH, Feng YL, Liu H, Guo Z, Zhang C. Preparation and evaluation of activated carbon with different polycondensed phosphorus oxyacids (H_3PO_4, $H_4P_2O_7$, $H_6P_4O_{13}$ and $C_6H_{18}O_{24}P_6$) activation employing mushroom roots as precursor. J Anal Appl Pyrol. 2014;19(5):41–46.
20. Sun YY, Yue QY, Gao BY, Huang L, Xing X, Qian L. Comparative study on characterization and adsorption properties of activated carbons with H_3PO_4 and $H_4P_2O_7$ activation employing Cyperus alternifolius as precursor. Chem Eng J. 2012;98:790–797.
21. Hafeez F, Amin BAZ, Akbar U, Iqbal A, Faridullah MB, Nazir R. Assessment of phosphorus availability in soil by introducing P-solubilizing novel bacterial and fungal strains of lower Himalaya. Commun Soil Sci Plant Anal. 2019;50(13):1541–1549.
22. Puziy AM, Poddubnaya OI, Martínez-Alonso A, Suárez-García F, Tascón JMD. Surface chemistry of phosphorus-containing carbons of lignocellulosic origin. Carbon. 2005;14(43):2857–2868.

23. Bi ZH, Li H, Kong QQ, Li F, Chen JP, Ahmad A, Wei X, Xie L, Chen C. Structural evolution of phosphorus species on graphene with a stabilized electrochemical interface. ACS Appl Mater Interfaces. 2019;11(12):1142–11430.
24. Qian TT, Yang Q, Jun DCF, Dong F, Zhou Y. Transformation of phosphorus in sewage sludge biochar mediated by a phosphate-solubilizing microorganism. Chem Eng J. 2019;359:1573–1580.
25. Valero-Romero MJ, García-Mateos FJ, Rodríguez-Mirasol J, Cordero T. Role of surface phosphorus complexes on the oxidation of porous carbons. Fuel Process Technol. 2017;157:116–126.
26. Liu YT, Li KX, Liu Y, Pu LT, Chen ZH, Deng SG. The high-performance and mechanism of P-doped activated carbon as a catalyst for air-cathode microbial fuel cells. J Mat Chem A. 2015;3(42):21149–21158.
27. Zhang JJ, Shao J, Jin QZ, Zhang X, Yang HP, Chen YQ. Effect of deashing on activation process and lead adsorption capacities of sludge-based biochar. Sci Total Environ. 2020;716(10):1–10.
28. Sun T, Xu YM, Sun YB, Wang L, Liang XF, Jia HT. Crayfish shell biochar for the mitigation of Pb contaminated water and soil: Characteristics, mechanisms, and applications. Environ Pollut. 2021;271:2–10.
29. Sahin O, Taskin MB, Kaya EC, Atakol O, Emir E, Inal A, Gunes A. Effect of acid modification of biochar on nutrient availability and maize growth in a calcareous soil. Soil Use Manag. 2017;3(33):447–456.
30. Taskin MB, Kadioglu YK, Sahin O, Inal A, Gunes A. Effect of acid modified biochar on the growth and essential and non-essential element content of bean, chickpea, soybean, and maize grown in calcareous soil. Commun Soil Sci Plant Anal. 2019;50(13):1604–1613.
31. Liu L, Li Y, Fan S. Preparation of KOH and H_3PO_4 Modified biochar and its application in methylene blue removal from aqueous solution. Processes. 2019;12:891–902.
32. Wei YQ, Wang J, Chang RX, Zhan YB, Wei D, Zhang L. Composting with biochar or woody peat addition reduces phosphorus bioavailability. Sci Total Environ. 2021;746:5–13.
33. Adhikari S, Gasco G, Mendez A, Surapaneni A, Jegatheesan V, Shah K, Paz-Ferreiro J. Influence of pyrolysis parameters on phosphorus fractions of biosolids derived biochar. Sci Total Environ. 2019;695:38–46.
34. Ahmad M, Usman ARA, Al-Faraj AS, Ahmad M, Sallam A, Al-Wabel MI. Phosphorus-loaded biochar changes soil heavy metals availability and uptake potential of maize (*Zea mays* L.) plants. Chemosphere. 2018;194:327–339.
35. Marks EAN, Alcañiz JM, Domene X. Unintended effects of biochars on short-term plant growth in a calcareous soil. Plant Soil. 2014;385(2):87–105.
36. Teng ZD, Zhu J, Shao W, Zhang K, Li M, Whelan MJ. Increasing plant availability of legacy phosphorus in calcareous soils using some phosphorus activators. J Environ Manage. 2020;256:52–58.
37. Liu XY, Yang JS, Tao JY, Yao RJ, Wang XP, Xie WP, Zhu H. Elucidating the effect and interaction mechanism of fulvic acid and nitrogen fertilizer application on phosphorus availability in a salt-affected soil. J Soils Sediments. 2021;21:2525–2539.
38. Cui HJ, Wang MK, Ming LF. Enhancing phosphorus availability in phosphorus-fertilized zones by reducing phosphate adsorbed on ferrihydrite using rice straw-derived biochar. J Soils Sediments. 2011;11(7):1135–1141.
39. Figueiredo CCD, Pinheiro TD, Oliveira LEZD, Araujo ASD, Coser TR, Paz-Ferreiro J. Direct and residual effect of biochar derived from biosolids on soil phosphorus pools: a four-year field assessment. Sci Total Environ. 2020;739(15):8–16.
40. Ghodszad L, Reyhanitabar A, Maghsoodi MR, Lajayer BA, Chang SX. Biochar affects the fate of phosphorus in soil and water: A critical review. Chemosphere. 2021;283(1): 131176.
41. Chen H, Feng Y, Yang X, Yang B, Sarkar B, Bolan N, Meng J, Wu F, Wong JWC, Chen W, Wang H. Assessing simultaneous immobilization of lead and improvement of phosphorus availability through application of phosphorus-rich biochar in a contaminated soil: a pot experiment. Chemosphere. 2022;296: 133891.

Publisher's Note